HHS Public Access

Author manuscript

Amyloid. Author manuscript; available in PMC 2022 March 01.

Published in final edited form as:

Amyloid. 2021 March ; 28(1): 24–29. doi:10.1080/13506129.2020.1808783.

Blinded potency comparison of transthyretin kinetic stabilizers by subunit exchange in human plasma

Luke T. Nelson[1], **Ryan J. Paxman**[1], **Jin Xu**[1], **Bill Webb**[2], **Evan T. Powers**[1,*], **Jeffery W. Kelly**[1,3,*]

[1]Department of Chemistry, The Scripps Research Institute, La Jolla, CA, USA

[2]Center for Metabolomics, The Scripps Research Institute, La Jolla, CA, USA

[3]The Skaggs Institute for Chemical Biology, The Scripps Research Institute, CA, USA

Abstract

Transthyretin (TTR) tetramer dissociation is rate limiting for aggregation and subunit exchange. Slowing of TTR tetramer dissociation via kinetic stabilizer binding slows cardiomyopathy progression. Quadruplicate subunit exchange comparisons of the drug candidate AG10, and the drugs tolcapone, diflunisal, and tafamidis were carried out at 1, 5, 10, 20 and 30 μM concentrations in 4 distinct pooled wild type TTR (TTRwt) human plasma samples. These experiments reveal that the concentration dependence of the efficacy of each compound at inhibiting TTR dissociation was primarily determined by the ratio between the stabilizer's dissociation constants from TTR and albumin, which competes with TTR to bind kinetic stabilizers. The best stabilizers, tafamidis (80 mg QD), AG10 (800 mg BID), and tolcapone (3 × 100 mg over 12 h), exhibit very similar kinetic stabilization at the plasma concentrations resulting from these doses. At a 10 μM plasma concentration, AG10 is slightly more potent as a kinetic stabilizer vs. tolcapone and tafamidis (which are similar), which are substantially more potent than diflunisal. Dissociation of TTR can be limited to 10% of its normal rate at concentrations of 5.7 μM AG10, 10.3 μM tolcapone, 12.0 μM tafamidis, and 188 μM diflunisal. The potency similarities revealed by our study suggest that differences in safety, adsorption and metabolism, pharmacokinetics, and tissue distribution become important for kinetic stabilizer clinical use decisions.

Keywords

Kinetic stabilization; Wild-type transthyretin (TTR) amyloid cardiomyopathy (ATTRwt-CM); hereditary transthyretin (TTR) amyloid cardiomyopathy (ATTRv-CM); senile systemic amyloidosis; transthyretin (TTR) central nervous system amyloidosis; amyloid angiopathy; leptomeningeal transthyretin (TTR) amyloidosis; vitreous transthyretin (TTR) amyloidosis; transthyretin (TTR) eye amyloidosis

[*]Corresponding authors: Jeffery W. Kelly, Department of Chemistry, The Scripps Research Institute, 10550 North Torrey Pines Road, La Jolla, CA 92037, USA. jkelly@scripps.edu. +1-858-784-9880; Evan T. Powers, Department of Chemistry, The Scripps Research Institute, 10550 North Torrey Pines Road, La Jolla, CA 92037, USA. epowers@scripps.edu. +1-858-784-9880.

Disclosure statement

JWK and ETP discovered tafamidis, receive sales royalties and sales milestone payments, thus the kinetic stabilizer comparison herein was conducted in a blinded fashion, and all participants only learned of the unblinding after seeing the blinded results.

Introduction

Wild type (wt) transthyretin (TTR) aggregation causes the disease wild type TTR amyloid cardiomyopathy (wtATTR-CM), previously called Senile Systemic Amyloidosis [1]. Patients with ATTRwt-CM present with a principal cardiomyopathy, along with compromised autonomic nervous system function [1, 2]. ATTRwt-CM is the most common of the transthyretin amyloidoses, affecting approximately 10% of the elderly male population [3, 4]. Hence, kinetic stabilizers—small molecules that bind to the native tetrameric structure of TTR preferably over the dissociative transition state, slowing dissociation and inhibiting aggregation—were compared herein in the context of wt TTR.

Rate-limiting dissociation of the native TTR tetramer, followed by monomer misfolding [5] enables formation of transthyretin aggregate structures [6–9]. Compelling genetic and pharmacologic evidence support the hypothesis that TTR aggregation into a spectrum of aggregate structures [10] drives the cardiomyopathy degenerative phenotypes, especially early in the disease course [9, 11–20].

The kinetic stabilizer tafamidis is the only drug approved by the regulatory agencies to slow the progression of the TTR cardiomyopathies (ATTRwt-CM and ATTRv-CM) [18]. Two other TTR kinetic stabilizers—the drug candidate, AG10, and the Parkinson's disease drug, tolcapone, are currently under consideration for treating the ATTR amyloidoses [21–27]. There are reports suggesting that AG10 and tolcapone are superior to tafamidis as TTR kinetic stabilizers [21, 26, 27]. Notably, these assessments are based on comparisons made under denaturing conditions, which can differentially reduce the binding affinity of the kinetic stabilizers to tetrameric TTR, making extrapolations to physiological conditions difficult. AG10 was assessed under acidic conditions in human plasma [21], whereas tolcapone was analyzed in human plasma to which urea was added [26]. In these assays, in the presence of a kinetic stabilizer candidate or just vehicle, and after an incubation period in plasma under denaturing conditions, TTR is subjected to glutaraldehyde cross-linking. The TTR tetramer preserved by kinetic stabilizer binding is then quantified either by SDS-PAGE / Western blot or by immunoturbidity (the basis for the clinical laboratory test for measuring TTR blood levels). The more tetramer present, the better the stabilizer performance under denaturing conditions [28].

Pharmacologic kinetic stabilization is defined by the decrease in the rate of TTR tetramer dissociation in human plasma in the presence of the kinetic stabilizer [29–32]. Wild type TTR subunit exchange in plasma allows for a direct comparison of different kinetic stabilizers under physiological conditions, because subunit exchange [33–35], like aggregation [5–7, 34–36], is rate limited by TTR tetramer dissociation. This assay quantifies kinetic stabilization in the complex plasma environment wherein TTR likely aggregates [20], in the presence of all plasma factors that influence TTR kinetic stability, those that are known [37, 38] and unknown.

Methods

A comprehensive Materials and methods section can be found in the on-line Supplemental Material for: Dual-FLAG-tagged WT TTR Expression and Purification, Plasma Preparation for Experiments 1 and 2, Processing the Peak Area Data, Global fits of Subunit Exchange Data, Kinetic Stabilizer Purity Assessments, Kinetic Stabilizer Concentration Determinations, Sample Blinding, and Study Approval.

Results

Measuring the rate of tetramer dissociation in human plasma by subunit exchange in the presence of a pharmacologic kinetic stabilizer allows one to assess the oral dose of a kinetic stabilizer required to slow TTR tetramer dissociation to a desired extent under physiological conditions [29, 30]. The desired extent is ultimately determined by placebo-controlled clinical trials (see Discussion).

In plasma, monomeric TTR subunits resulting from tetramer dissociation predominantly reassemble back to tetramers—a process that is not normally detectable [29]. However, if recombinant dual-FLAG-tagged wt TTR (FT_2-WT TTR) homotetramers (comprising the red subunits in Figure 1A) are added to plasma, the concurrent dissociation of endogenous untagged tetrameric plasma TTR (3–5 μM; represented by green subunits) and FT_2-WT TTR tetramers (final concentration of 1 μM) results in a solution of tagged and untagged monomeric TTR subunits [29] (Figure 1A). When these monomers come together during the process of tetramer reassembly, heterotetramers 2, 3 and 4 made up of the tagged TTR subunits and endogenous TTR subunits are afforded in ratios approximated by the binomial distribution (Figure 1A) [33]. The final concentration of homotetramers 1 and 5 are predicted analogously. Slight deviations from the expected binomial distribution are due to the homo- and heterotetramers depicted in Figure 1A not being perfectly isoenergetic [29, 32, 33].

To facilitate TTR tetramer detection in plasma, in the context of thousands of additional proteins and biomolecules, we employed the fluorogenic TTR-modifying small molecule A2 (Figure 1B) [39]. Small molecule A2 binds rapidly to natively folded tetrameric TTR, arresting any further subunit exchange, yielding the non-fluorescent TTR•$(A2)_2$ complexes of tetramers 1–5 (Figure 1B; left panel). Once bound, A2 chemoselectively reacts with two of the four TTR subunits in the TTR tetramer, acylating the Lys-15 ε-amino groups in the thyroxine binding sites, rendering the TTR-$(A2\ fragment)_2$ covalent conjugates of tetramers 1–5 fluorescent (Figure 1B; right panel). Because the N-terminal dual-FLAG tag does not affect the A2 binding site, using the FLAG-tagged TTR allows for equal fluorescence detection of tetramers 1–5. The additional negative charges contributed by each TTR subunit harboring a dual-FLAG tag (red subunits) in a tetramer allows for ultraperformance liquid chromatography (UPLC) quaternary ammonium anion exchange chromatography separation of tetramers 1–5 in plasma, enabling fluorescence detection-based quantification of TTR-$(A2\ fragment)_2$ of tetramers 1–5 (Figure 1C) as a function of the subunit exchange period to generate subunit exchange kinetics [29].

In “experiment 1” we performed blinded subunit exchange comparisons of the drug candidate AG10, and the drugs tolcapone, diflunisal, and tafamidis at 30, 20, 10, 5, and 1 μM concentrations in 3 pooled human plasma samples, each derived from three distinct donors (Supplemental Figure S1; the TTR in these plasma samples is likely to be WT, given that the donors were healthy). In all cases, we calculated the fraction of exchange at each time point based on the extent to which tetramer 3 (Figure 1A) had approached its expected final value. Previous work has shown that, at least for exchange between WT TTR and FT_2-WT TTR, the rates of appearance / disappearance of the other four tetramers (tetramers 1, 2, 4, and 5 in Figure 1A) are similar to that of tetramer 3 [29]. AG10 is slightly more potent as a kinetic stabilizer vs. tolcapone and tafamidis which exhibit similar potency (Table 1; Supplemental Figure S1). Notably, the differences between these kinetic stabilizers become very small at the pharmacologically relevant upper end of the concentration range tested. The concentration of the TTR kinetic stabilizers being compared were quantified by three independent methods to be sure that accurate concentrations were employed in the subunit exchange experiments (see methods in the Supplemental Material for details). Strictly analogous results were obtained in “experiment 2” employing two technical replicates with a single pooled plasma sample generated from six healthy donors (Table 1; Supplemental Figure S2). In both experiments we used freshly prepared kinetic stabilizer solutions.

To further scrutinize the efficacies of tafamidis, AG10, tolcapone, and diflunisal for inhibiting TTR dissociation in blood plasma, we fitted the data from experiments 1 and 2 to a model for TTR subunit exchange in the presence of kinetic stabilizers and a competing kinetic stabilizer-binding protein; in this case, albumin (Figure 2). We have shown previously that subunit exchange is well approximated as a monoexponential process with an apparent rate constant $k_{ex} = f_{unbound} \times k_{diss}$, where $f_{unbound}$ is the fraction of TTR with no ligands bound and k_{diss} is the intrinsic TTR tetramer dissociation rate constant [31, 33]. The parameter $f_{unbound}$ is a function of a compound’s affinity for TTR’s two binding sites (K_{d1}, K_{d2}) as well as its affinity for albumin ($K_{d,Alb}$), as discussed in the Supplemental Methods section. Values for K_{d1} and K_{d2} have been reported for each kinetic stabilizer compared in our study: tafamidis, K_{d1} = 3.1 nM, K_{d2} = 238 nM (average values from [40] and [31]); AG10, K_{d1} = 4.8 nM, K_{d2} = 314 nM [40]; tolcapone, K_{d1} = 41 nM, K_{d2} = 4.3 μM [41]; diflunisal, K_{d1} = 75 nM, K_{d2} = 1.1 μM [8]. Thus, K_{d1} and K_{d2} were used as fixed paramters in the global fit, while k_{diss} and $K_{d,Alb}$ were allowed to vary to optimize the fits to the data.

The fits to the data from experiment 1 were uniformly good, with $R^2 > 0.98$ for each kinetic stabilizer (Supplemental Figure S1). Similarly, the fits to the data from experiment 2 yielded $R^2 > 0.96$ for each small molecule (Supplemental Figure S2). The fits to the combined data from experiments 1 and 2 yielded an $R^2 > 0.96$ as well (Figure 2). The apparent subunit exchange rates, k_{ex}, resulting from the fits from each subunit exchange time course at each small molecule concentration are listed in Table 1. The data in the second column is for experiment 1 (biological triplicate data), the data in the third column is for experiment 2 (technical duplicate data), and the data in the fourth column derives from fitting the combined data from experiments 1 and 2 (five replicates). For each concentration of each stabilizer, the rate constants in the three columns are very similar, with an average relative standard deviation of 6.6%, superior to kinetic stabilizer comparisons made under denaturing conditions discussed in the Introduction section, wherein the relative standard

deviation is substantially higher than 6.6%. Importantly, the best-fit subunit exchange rates, k_{ex}, from the global fit to the data for each kinetic stabilizer are very similar to the k_{ex} values derived from individually analyzing experiment 1 or experiment 2, demonstrating the reproducibility of the subunit exchange method in Table 1 (cf. the k_{ex} derived from the aforementioned global fits in columns 2, 3 and 4). Moreover, it is clear that the less labor-intensive experiment 2 carried out in duplicate with one pooled plasma sample from 6 donors is sufficient for comparing kinetic stabilizer potencies (Table 1) using WT TTR subunit exchange rates, cf. Supplemental Figure S1 to Supplemental Figure S2.

The global fit to the combined dataset from experiments 1 and 2 revealed that the fundamental TTR dissocation rate constant, k_{diss}, in the absence of any kinetic stabilizer is ≈ 0.0149 h^{-1} (this quantity was determined separately using the data from each small molecule as follows: tafamidis, k_{diss} = 0.0140 ± 0.0007 h^{-1}; AG10, k_{diss} = 0.0147 ± 0.009 h^{-1}; tolcapone, k_{diss} = 0.0153 ± 0.0007 h^{-1}; diflunisal, k_{diss} = 0.0155 ± 0.0009 h^{-1}). The global fit of the data from experiments 1 and 2 to the aforementioned model also affords values for $K_{d,Alb}$ that were all in the low- to mid-micromolar range (tafamidis, $K_{d,Alb}$ = 1.8 ± 0.1 μM; AG10, $K_{d,Alb}$ = 9.5 ± 0.8 μM; tolcapone, $K_{d,Alb}$ = 32 ± 2 μM; diflunisal, $K_{d,Alb}$ = 1.2 ± 0.1 μM). Given these values, it appears that the primary determinant of a compound's efficacy at a given concentration for inhibiting TTR tetramer dissociation in blood plasma is the spread between its K_{d1} for binding to TTR and $K_{d,Alb}$. These decrease in the order AG10 ($K_{d,Alb}$ / K_{d1} = 1980) > tolcapone ($K_{d,Alb}$ / K_{d1} = 780) > tafamidis ($K_{d,Alb}$ / K_{d1} = 580) > diflunisal ($K_{d,Alb}$ / K_{d1} = 16). Given the value of k_{diss} for TTR and the values of K_{d1}, K_{d2}, and $K_{d,Alb}$ for the stabilizing compounds obtained from the fits, we calculate that dissociation of TTR can be limited to 10% of its normal rate at concentrations of 5.7 μM AG10, 10.3 μM tolcapone, 12.0 μM tafamidis, and 188 μM diflunisal. TTR dissociation could be further diminished to 3% of its normal rate at concentrations of 11.5 μM AG10, 25.9 μM tolcapone, 30.1 μM tafamidis, and 328 μM diflunisal, all of which are pharmacologically achievable plasma concentrations with oral dosing.

Discussion

It remains unclear what the minimal reduction in the rate of TTR tetramer dissociation is to achieve maximal clinical benefit, although TTR amyloidosis clinical trials and large clinical studies have put some constraints on this. We have previously reported data showing that slowing (36% of patients; n=76) or cessation of progression (34 % of patients; n=72) has been observed in hereditary TTRV30M polyneuropathy (ATTRv-PN) with tafamidis treatment (20 mg QD) [42], a clinical result associated with a mean tafamidis plasma concentration in these patients after 12 months of dosing of ≈ 9 μM. This concentration of tafamidis, assuming it is the same in ATTRwt-CM patients at the 20 mg QD dose, would be expected to slow the rate of wt TTR tetramer dissociation to ~14% of normal based on the subunit exchange data presented herein. Increasing the dose of tafamidis to 80 mg once daily (which yields a mean peak plasma concentration of ≈ 28 μM), lowers the rate of wt TTR tetramer dissociation to ~3% of normal in our experiments (61 mg Vyndamax formulation affords the same plasma concentration) [43]. Slowing of progression of ATTRv-PN has been observed with diflunisal treatment (250 mg BID), but we lack good information on plasma concentrations. Chronic dosing with 20 vs 80 mg of tafamidis decreases the wt TTR

dissociation rate from ≈ 14 % of normal to 3% of normal, as noted above, and the higher dose appears to offer a survival benefit over the lower dose after 51 months of observation (European Socity Cardiology June 2020 presentation).

It is clear that any arbitrary level of TTR kinetic stabilization can be achieved by a given small molecule kinetic stabilizer through simply adjusting the plasma concentration, which in turn can be controlled via the oral dose, safety attributes permitting. If a reduction to ≤ 4 % of the normal wt TTR tetramer dissociation rate is desired, this would require a daily oral dose of 1600 mg of AG10 to afford a mean peak plasma concentration of ≈ 11 μM, or a daily oral dose of 80 mg of tafamidis to achieve a mean peak plasma concentration of ≈ 28 μM, as demonstrated by the data above. Even diflunisal is a very effective kinetic stabilizer at the ≈ 100 – 200 μM concentration achieved by a daily oral dose of 500 mg, demonstrating that even large potency differences can be overcome by very good oral bioavailability, a good half-life and the lack of substantial plasma metabolites, along with modest albumin binding.

Conclusion and Perspective.

Sixteen hundred mg of AG10 daily and 80 mg of tafamidis daily reduce the rate of WT TTR tetramer dissociation by ≥ 96% at mean peak plasma concentrations of ≈ 11 μM and ≈ 28 μM, respectively. While AG10 is 4 times more potent than tafamidis at a fixed plasma concentration (e.g., 10 μM; Table 1), the combination of AG10's half-life of 25 h vs 49 h for tafamidis, modest AG10 oral bioavailability, and the substantial metabolism of AG10 of ≈ 33 % (acylglucuronidate) vs ≤ 10% for tafamidis, requires that 20 times more AG10 needs to be orally administered than tafamidis to afford the same wt TTR kinetic stabilization. Tolcapone's black box warning aside, its 3 h half-life makes it very challenging to find a tolcapone dose and dosing regimen that can match the kinetic stabilization imparted by other stabilizers during the sleep cycle [26]. The potency similarities revealed by our study suggest that other pharmacologic considerations, such as safety, adsorption and metabolism, pharmacokinetics, and the stabilizers' tissue distribution (tafamidis and tolcapone have meaningful exposure in the eyes and in the brain [44, 45]) are also very important considerations for clinical use decisions.

Supplementary Material

Refer to Web version on PubMed Central for supplementary material.

Acknowledgments

We thank Dr. Marcus Jaeger for insightful comments on the manuscript. The discovery of tafamidis and the repurposing of diflunisal for the ATTR amyloidoses would not have been possible without sustained NIH funding of the Kelly Laboratory from DK 046335. We thank Colleen Fearns Ph.D. for scientific insights and sophisticated editing of the text and The Scripps Research Institute's Normal Blood Donor Services Center for enabling us to procure plasma.

Abbreviations

BID	twice a day

CNS	central nervous system
CSF	cerebrospinal fluid
FT_2-TTR	dual-FLAG-tagged TTR
ATTRv-CM	hereditary TTR amyloid cardiomyopathy
ATTRv-PN	hereditary TTR amyloidosis with polyneuropathy
HPLC	high performance liquid chromatography
PNS	peripheral nervous system
QD	once a day
TTR	transthyretin
UPLC	ultra-performance liquid chromatography
VB	vitreous body
wt	wild-type
ATTRwt-CM	wild-type transthyretin amyloid cardiomyopathy

References

1. Westermark P, Sletten K, Johansson B, et al. Fibril in senile systemic amyloidosis is derived from normal transthyretin. Proc Natl Acad Sci U S A. 1990;87:2843–2845. [PubMed: 2320592]
2. Ruberg FL, Grogan M, Hanna M, et al. Transthyretin amyloid cardiomyopathy JACC State-of-the-Art Review. J Am Coll Cardiol. 2019;73:2872–2891. [PubMed: 31171094]
3. Ueda M, Horibata Y, Shono M, et al. Clinicopathological features of senile systemic amyloidosis: an ante- and post-mortem study. Mod Pathol. 2011;24:1533–1544. [PubMed: 21822203]
4. Tanskanen M, Peuralinna T, Polvikoski T, et al. Senile systemic amyloidosis affects 25% of the very aged and associates with genetic variation in alpha2-macroglobulin and tau: A population-based autopsy study. Ann Med. 2008;40:232–239. [PubMed: 18382889]
5. Jiang X, Smith CS, Petrassi HM, et al. An engineered transthyretin monomer that is nonamyloidogenic, unless it is partially denatured. Biochemistry. 2001;40:11442–11452. [PubMed: 11560492]
6. Colon W, Kelly JW. Partial denaturation of transthyretin is sufficient for amyloid fibril formation in vitro. Biochemistry. 1992;31:8654–8660. [PubMed: 1390650]
7. Lai Z, Colon W, Kelly JW. The acid-mediated denaturation pathway of transthyretin yields a conformational intermediate that can self-assemble into amyloid. Biochemistry. 1996;35:6470–6482. [PubMed: 8639594]
8. Hammarstrom P, Wiseman RL, Powers ET, et al. Prevention of transthyretin amyloid disease by changing protein misfolding energetics. Science. 2003;299:713–716. [PubMed: 12560553]
9. Hammarstrom P, Schneider F, Kelly JW. Trans-suppression of misfolding in an amyloid disease. Science. 2001;293:2459–2462. [PubMed: 11577236]
10. Eisele YS, Monteiro C, Fearns C, et al. Targeting protein aggregation for the treatment of degenerative diseases. Nat Rev Drug Disc. 2015;14:759–780.
11. Coelho T, Carvalho M, Saraiva MJ, et al. A strikingly benign evolution of FAP in an individual found to be a compound heterozygote for two TTR mutations: TTR MET 30 and TTR MET 119. J Rheumatol. 1993;20:179.

12. Coelho T, Maia LF, Martins dSA, et al. Tafamidis for transthyretin familial amyloid polyneuropathy: A randomized, controlled trial. Neurology. 2012;79:785–792. [PubMed: 22843282]
13. Coelho T, Maia LF, da Silva AM, et al. Long-term effects of tafamidis for the treatment of transthyretin familial amyloid polyneuropathy. J Neurol. 2013;260:2802–2814. [PubMed: 23974642]
14. Coelho T, Ines M, Conceicao I, et al. Natural history and survival in stage 1 Val30Met transthyretin familial amyloid polyneuropathy. Neurology. 2018; 91:E1999–E2009. [PubMed: 30333157]
15. Berk JL, Suhr OB, Obici L, et al. Repurposing diflunisal for familial amyloid polyneuropathy a randomized clinical trial. JAMA. 2013;310:2658–2667. [PubMed: 24368466]
16. Benson MD, Waddington-Cruz M, Berk JL, et al. Inotersen treatment for patients with hereditary transthyretin amyloidosis. N Eng J Med. 2018;379:22–31.
17. Adams D, Gonzalez-Duarte A, O'Riordan WD, et al. Patisiran, an RNAi therapeutic, for hereditary transthyretin amyloidosis. N Engl J Med. 2018;379:11–21. [PubMed: 29972753]
18. Maurer MS, Schwartz JH, Gundapaneni B, et al. Tafamidis treatment for patients with transthyretin amyloid cardiomyopathy. N Eng J Med. 2018;379:1007–1016.
19. Rosenblum H, Castano A, Alvarez J, et al. TTR (transthyretin) stabilizers are associated with improved survival in patients with ttr cardiac amyloidosis. Circulation-Heart Fail. 2018;11.
20. Schonhoft JD, Monteiro C, Plate L, et al. Peptide probes detect misfolded transthyretin oligomers in plasma of hereditary amyloidosis patients. Science Transl Med. 2017;9.
21. Judge DP, Heitner SB, Falk RH, et al. Transthyretin stabilization by AG10 in symptomatic transthyretin amyloid cardiomyopathy. J Am Coll Cardiol. 2019;74:285–295. [PubMed: 30885685]
22. Fox JC, Heitner S, Falk R, et al. AG10 consistently stabilizes transthyretin to a high level in both wild type and mutant amyloid cardiomyopathy: responder analyses from a phase 2 clinical trial. J Am Coll Cardiol. 2019;73:660–660.
23. Fox JC, Hellawell JL, Rao S, et al. First-in-human study of AG10, a Novel, oral, specific, selective, and potent transthyretin stabilizer for the treatment of transthyretin amyloidosis: a phase 1 safety, tolerability, pharmacokinetic, and pharmacodynamic study in healthy adult volunteers. Clin Pharmacol Drug Dev. 2019;9:115–129. [PubMed: 31172685]
24. Hellawell JL, Rao S, O'Reilly T, et al. AG10, A novel, potent and selective transthyretin stabilizer, is well tolerated at doses resulting in target therapeutic blood levels, and demonstrates clinical proof-of-concept in healthy volunteers. J Card Fail. 2018;24:S31–S32.
25. Sinha U, Rao SI, Fox J, et al. AG10 potently and selectively stabilizes transthyretin in vitro and upon oral dosing in dogs: potential for treating transthyretin amyloidosis. Circulation. 2017; 136.
26. Gamez J, Salvad M, Reig N, et al. Transthyretin stabilization activity of the catechol-O-methyltransferase inhibitor tolcapone (SOM0226) in hereditary ATTR amyloidosis patients and asymptomatic carriers: proof-of-concept study. Amyloid. 2019;26:74–84. [PubMed: 31119947]
27. Sant'Anna R, Gallego P, Robinson LZ, et al. Repositioning tolcapone as a potent inhibitor of transthyretin amyloidogenesis and associated cellular toxicity. Nat Commun. 2016; 7: 10787 [PubMed: 26902880]
28. Sekijima Y, Dendle MA, Kelly JW. Orally administered diflunisal stabilizes transthyretin against dissociation required for amyloidogenesis. Amyloid. 2006;13:236–249. [PubMed: 17107884]
29. Rappley I, Monteiro C, Novais M, et al. Quantification of transthyretin kinetic stability in human plasma using subunit exchange. Biochemistry. 2014;53:1993–2006. [PubMed: 24661308]
30. Cho Y, Baranczak A, Helmke S, et al. Personalized medicine approach for optimizing the dose of tafamidis to potentially ameliorate wild-type transthyretin amyloidosis (cardiomyopathy). Amyloid. 2015;22:175–180. [PubMed: 26193961]
31. Bulawa CE, Connelly S, DeVit M, et al. Tafamidis, a potent and selective transthyretin kinetic stabilizer that inhibits the amyloid cascade. Proc Natl Acad Sci U S A. 2012;109:9629–9634, S9629/9621-S9629/9629. [PubMed: 22645360]
32. Schneider F, Hammarstrom P, Kelly JW. Transthyretin slowly exchanges subunits under physiological conditions: A convenient chromatographic method to study subunit exchange in oligomeric proteins. Protein Sci. 2001;10:1606–1613. [PubMed: 11468357]

33. Wiseman RL, Green NS, Kelly JW. Kinetic stabilization of an oligomeric protein under physiological conditions demonstrated by a lack of subunit exchange: implications for transthyretin amyloidosis. Biochemistry. 2005;44:9265–9274. [PubMed: 15966751]
34. Foss TR, Kelker MS, Wiseman RL, et al. Kinetic stabilization of the native state by protein engineering: implications for inhibition of transthyretin amyloidogenesis. J Mol Biol. 2005;347:841–854. [PubMed: 15769474]
35. Foss TR, Wiseman RL, Kelly JW. The pathway by which the tetrameric protein transthyretin dissociates. Biochemistry. 2005;44:15525–15533. [PubMed: 16300401]
36. Hurshman AR, White JT, Powers ET, et al. Transthyretin aggregation under partially denaturing conditions is a downhill polymerization. Biochemistry. 2004;43:7365–7381. [PubMed: 15182180]
37. White JT, Kelly JW. Support for the multigenic hypothesis of amyloidosis: the binding stoichiometry of retinol-binding protein, vitamin A, and thyroid hormone influences transthyretin amyloidogenicity in vitro. Proc Natl Acad Sci U S A. 2001;98:13019–13024. [PubMed: 11687657]
38. Arvanitis M, Simon S, Chan G, et al. Retinol binding protein 4 (RBP4) concentration identifies V122I transthyretin cardiac amyloidosis. Amyloid. 2017;24:120–121. [PubMed: 28434357]
39. Choi S, Ong DS, Kelly JW. A stilbene that binds selectively to transthyretin in cells and remains dark until it undergoes a chemoselective reaction to create a bright blue fluorescent conjugate. J Am Chem Soc. 2010;132:16043–16051. [PubMed: 20964336]
40. Penchala SC, Connelly S, Wang Y, et al. AG10 inhibits amyloidogenesis and cellular toxicity of the familial amyloid cardiomyopathy-associated V122I transthyretin. Proc Natl Acad Sci U S A. 2013;110:9992–9997. [PubMed: 23716704]
41. Robinson LZ, Reixach N. Quantification of quaternary structure stability in aggregation-prone proteins under physiological conditions: the transthyretin case. Biochemistry. 2014;53:6496–6510. [PubMed: 25245430]
42. Monteiro C, Mesgazardeh JS, Anselmo J, et al. Predictive model of response to tafamidis in hereditary ATTR polyneuropathy. JCI Insight. 2019;4:e126526.
43. Lockwood PA, Le VH, O'Gorman MT, et al. The bioequivalence of tafamidis 61-mg free acid capsules and tafamidis meglumine 4 × 20-mg capsules in healthy volunteers. Clin Pharmacol Drug Dev. 2020; DOI: 10.1002/cpdd.789.
44. Monteiro C, da Silva AM, Ferreira N, et al. Cerebrospinal fluid and vitreous body exposure to orally administered tafamidis in hereditary ATTRV30M (p.TTRV50M) amyloidosis patients. Amyloid. 2018;25:120–128. [PubMed: 29993288]
45. Russ H, Muller T, Woitalla D, et al. Detection of tolcapone in the cerebrospinal fluid of parkinsonian subjects. Naunyn-Schmiedebergs Arch Pharmacol. 1999;360:719–720. [PubMed: 10619191]

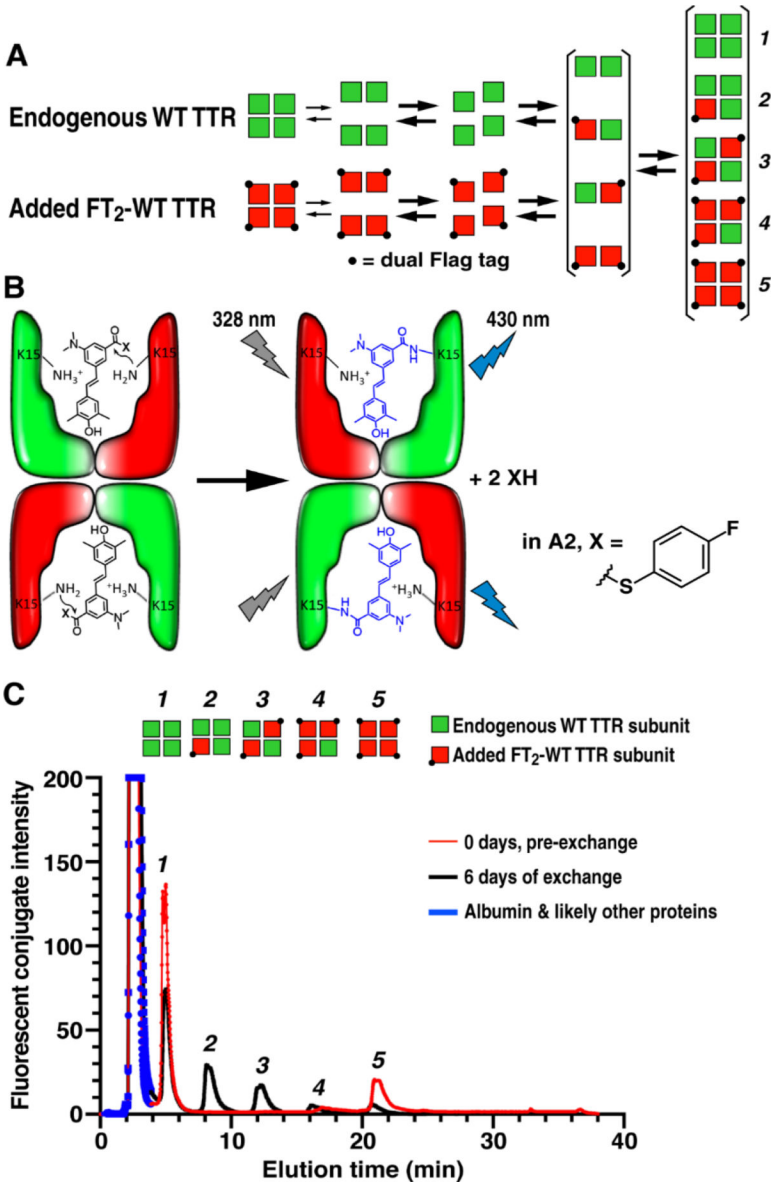

Figure 1. Subunit Exchange to Quantify TTR Tetramer Kinetic Stability.

(A) Schematic of the steps involved in subunit exchange between endogenous TTR in human plasma represented by green subunits and added dual-FLAG tagged WT TTR (FT_2-WT TTR) depicted by red subunits. Rate-limiting tetramer dissociation depleting homotetramers **1** and **5**, and subunit re-association to afford heterotetramers **2**, **3** and **4** allow the apparent rate constants for subunit exchange (k_{ex}) to be determined. (B) Aliquots removed as a function of time are removed from the subunit exchange reaction and injected into an excess of **A2**, which binds to the two binding sites in TTR and then reacts with the Lys-15 residues, rendering the TTR conjugates detectable by fluorescence in the background of the 4000+ proteins comprising plasma. (C) Ion exchange chromatography of whole human plasma with fluorescence detection can be used to follow the abundances of tetramers **1-5** as a function of time, yielding the time courses in Figure 2 and Supplemental

Figures S1 and S2, which can be fit to determine k_{ex} as a function of the concentration of various kinetic stabilizers.

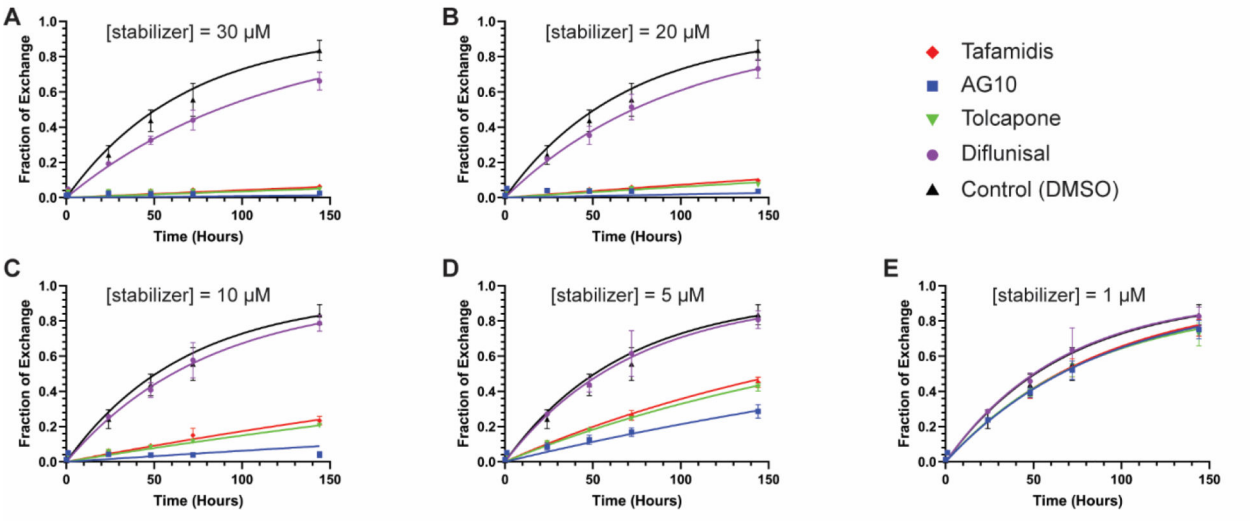

Figure 2. TTR subunit exchange kinetics in the presence of kinetic stabilizers at varying concentrations, experiments 1 and 2 combined.

Time courses of subunit exchange between endogenous plasma TTR (~ 3 μM) and added dual-flag-tagged WT-TTR (1 μM) in the presence of kinetic stabilizers at the indicated concentrations. Data from experiments 1 and 2 were combined and fit globally. The x-axis shows time in hours; the y-axis shows the fraction of exchange as calculated from the area under peak 3 in ion exchange chromatograms (see Figure 1C for a sample chromatogram and the Materials and Methods for the procedure to calculate fraction exchange). (A) Subunit exchange time courses in the presence of kinetic stabilizers at a concentration of 30 μM. (B) As in panel A, but at a stabilizer concentration = 20 μM. (C) As in panel A, but at a stabilizer concentration = 10 μM. (D) As in panel A, but at a stabilizer concentration = 5 μM. (E) As in panel A, but at a stabilizer concentration = 1 μM. The same DMSO control time course is shown in each plot. Red diamonds = tafamidis; blue squares = AG10; inverted green triangle = tolcapone; purple circle = diflunisal; black triangle = DMSO control. Data points represent the mean and error bars the standard deviation of the combined data set from experiments 1 and 2. The curves in each plot represent the best fits to the combined data based on the model described in the text.

Table 1.

Apparent k_{ex} at all ligand concentrations calculated based on the fits to the subunit exchange data from experiment 1, experiment 2, and the combined data.

Kinetic Stabilizer	**Concentration (μM)**	**apparent k_{ex}, Experiment 1 (h^{-1})**	**apparent k_{ex}, Experiment 2 (h^{-1})**	**apparent k_{ex}, Combined Experiments (h^{-1})**
Tafamidis	0	0.0142	0.0140	0.0140
	1	0.0116	0.0115	0.0114
	5	0.0046	0.005	0.0046
	10	0.0020	0.0023	0.0020
	20	0.0008	0.0009	0.0008
	30	0.0004	0.0005	0.0004
AG10	0	0.0148	0.0164	0.0147
	1	0.0114	0.0129	0.0114
	5	0.0022	0.0037	0.0026
	10	0.0005	0.0012	0.0007
	20	0.0001	0.0004	0.0002
	30	0.0001	0.0002	0.0001
Tolcapone	0	0.0153	0.0157	0.0152
	1	0.0123	0.0127	0.0123
	5	0.0044	0.005	0.0045
	10	0.0017	0.0021	0.0018
	20	0.0007	0.0008	0.0007
	30	0.0004	0.0005	0.0004
Diflunisal	0	0.0156	0.0141	0.0155
	1	0.0153	0.0139	0.0151
	5	0.0142	0.0129	0.0139
	10	0.0129	0.0118	0.0126
	20	0.0109	0.0100	0.0104
	30	0.0093	0.0086	0.0088